

# Functional MRI of imprinting memory: a new avenue for neurobiology of early learning

Mehdi Behroozi

[mehdi.behroozi@ruhr-uni-bochum.de](mailto:mehdi.behroozi@ruhr-uni-bochum.de)

Ruhr Universität Bochum <https://orcid.org/0000-0001-8373-6168>

Elena Lorenzi

Center for Mind/Brain Sciences, University of Trento <https://orcid.org/0000-0001-8670-4751>

Sepideh Tabrik

Martin Tegenthoff

Alessandro Gozzi

Istituto Italiano di Tecnologia <https://orcid.org/0000-0002-5731-4137>

Onur Güntürkün

Ruhr University Bochum <https://orcid.org/0000-0003-4173-5233>

Giorgio Vallortigara

University of Trento <https://orcid.org/0000-0001-8192-9062>

---

## Article

**Keywords:** fMRI, imprinting, brain, learning, memory acquisition, retrieval

**Posted Date:** March 4th, 2024

**DOI:** <https://doi.org/10.21203/rs.3.rs-3970041/v1>

**License:**  This work is licensed under a Creative Commons Attribution 4.0 International License.

[Read Full License](#)

**Additional Declarations:** There is **NO** Competing Interest.

---

1     **Functional MRI of imprinting memory: a new avenue**  
2                     **for neurobiology of early learning**

3             *Mehdi Behroozi<sup>1,5\*</sup>, Elena Lorenzi<sup>2,5\*</sup>, Sepideh Tabrik<sup>3</sup>, Martin Tegenthoff<sup>3</sup>, Alessandro*  
4 *Gozzi<sup>4</sup>, Onur Güntürkün<sup>1</sup>, Giorgio Vallortigara<sup>2</sup>*

5             <sup>1</sup>Institute of Cognitive Neuroscience, Department of Biopsychology, Faculty of Psychology,  
6 Ruhr University Bochum, Universitätsstraße 150, 44780, Bochum, Germany

7             <sup>2</sup>Center for Mind/Brain Sciences, University of Trento, Piazza Manifattura 1, 38068  
8 Rovereto (TN), Italy

9             <sup>3</sup>Department of Neurology, BG-University Hospital Bergmannsheil, Ruhr-University  
10 Bochum, Bürkle-de-la-Camp-Platz 1, 44789, Bochum, Germany

11            <sup>4</sup> Functional neuroimaging laboratory, Istituto Italiano di Tecnologia, Rovereto, Italy

12            <sup>5</sup>These authors contributed equally to this work.

13            \* Corresponding authors: [mehdi.behroozi@ruhr-uni-bochum.de](mailto:mehdi.behroozi@ruhr-uni-bochum.de); [elena.lorenzi@unitn.it](mailto:elena.lorenzi@unitn.it);

14  
15  
16  
17  
18  
19  
20  
21  
22  
23  
24  
25  
26  
27  
28  
29  
30  
31  
32  
33  
34

## **Abstract**

Filial imprinting, a crucial ethological paradigm, provides insights into the neurobiology of early learning and its long-term impact on behaviour. To date, only invasive techniques, such as autoradiography or lesion, have been employed to understand this behaviour. The primary limitation of these methods lies in their constrained access to the entire brain, impeding the exploration of brain networks crucial at various stages of this paradigm. Recently, advances in functional magnetic resonance imaging (fMRI) in the avian brain have opened new windows to explore bird's brain function at the network level. Here, we developed a ground-breaking non-invasive functional MRI technique for awake, newly hatched chicks that record whole-brain BOLD signal changes throughout imprinting experiments. While the initial phases of memory acquisition imprinting behaviour have been unravelled, the long-term storage and retrieval components of imprinting memories are still unknown. Our findings identified potential long-term storage of imprinting memories across a neural network, including the hippocampal formation, the medial striatum, the arcopallium, and the prefrontal-like nidopallium caudolaterale. This platform opens up new avenues for exploring the broader landscape of learning and memory processes in neonatal vertebrates, contributing to a more comprehensive understanding of the intricate interplay between behaviour and brain networks.

**Keywords:** fMRI; imprinting; brain; learning; memory acquisition; retrieval.

## 35 Introduction

36 Filial imprinting is a learning process by which the young of some organisms can  
37 learn about a conspicuous object, usually the mother or siblings, by simply being exposed  
38 to it for a short period of time soon after birth<sup>1</sup>. It owes its great popularity to the work of  
39 Nobel-prize-winning ethologist Konrad Lorenz<sup>2</sup>, but it was originally described by Douglas  
40 Spalding<sup>3</sup> in the offspring of some nidifugous (precocial) bird species, such as chicks or  
41 ducklings (see <sup>4</sup>). Visual imprinting has been mostly studied, though acoustic or olfactory  
42 imprinting can be observed as well, the latter being prominent in mammals<sup>5</sup>.

43 Although in principle visual imprinting can occur with any kind of object, research  
44 has shown that the process is actually assisted by a set of biological predispositions which  
45 guides an animal's attention towards those object features that are more likely to be  
46 observed in social partners - e.g., preferences in domestic chicks include simple features  
47 such red colour (which is prominently observed in the head region of conspecifics), or  
48 self-propelled motion (which is typical of living things), as well as more complex assembly  
49 of features such as face-like stimuli or biological motion in point-light displays (review in  
50 <sup>4,6</sup>). Brain research has shown that biological predispositions are associated with the  
51 activation of areas of the so-called *Social Behavior Network*, and in particular of the lateral  
52 septum for motion stimuli and of the nucleus taenia (homologous of the mammalian  
53 medial amygdala<sup>7</sup>) for face-like stimuli (review in<sup>6</sup>).

54 Interest in filial imprinting quickly spanned from behavioural biology to psychological  
55 development and psychopathology, inspiring, for instance, John Bowlby's theory of  
56 attachment, which postulates a crucial role of the mother-child bond for subsequent

57 psychological development and, complementarily, the psychiatric outcomes associated  
58 with early mother deprivation (recent reviews in <sup>8,9</sup>).

59 In the 70's filial imprinting served as a model for the neurobiological investigation of  
60 memory. Gabriel Horn and colleagues (review in <sup>10</sup>) identified an associative brain region  
61 involved in the formation of an imprinting memory, the intermediate medial mesopallium  
62 (IMM according to the new avian brain nomenclature; previously referred to as IMHV,  
63 intermediate medial hyperstriatum ventrale<sup>11,12</sup>). IMM proved to be crucial during the  
64 acquisition phase of the visual imprinting memory. More precisely, it was found that  
65 exposure to the imprinting object was associated with changes in the left but not in the  
66 right IMM<sup>13,14</sup>. Subsequent studies with auditory imprinting revealed that the imprinting-  
67 related area extended ventrally into a medialmost nidopallial area, the nidopallium medial  
68 pars medialis (NMm)<sup>15,16</sup>. Here we will use the label medial nidopallium/mesopallium  
69 (MNM) to jointly label the mesopallial and nidopallial entity of the imprinting area.

70 Experiments involving sequential lesions, first to one side of IMM and subsequently  
71 to the other<sup>17,18</sup>, suggested that the store in the left IMM is only temporary, and the right  
72 IMM is implicated in transferring information from the left IMM to another, unknown brain  
73 region dubbed S', and that this transfer appears to be complete within 6 h after the end  
74 of exposure<sup>19</sup>. Thus, to cite Gabriel Horn's words "*We are still some ways from being able*  
75 *to visualize, through the microscope or by using brain imaging techniques, the neural*  
76 *trace of (imprinting) memory*"<sup>10</sup>. To overcome the technical limitations, recent  
77 advancements in functional magnetic resonance imaging (fMRI) turned it into a  
78 cornerstone neuroscientific technique. This powerful, non-invasive procedure serves as  
79 an indirect measure of neuronal activity throughout the entire brain, offering a

80 comprehensive perspective at the network level. It appears particularly well-suited to  
81 finally find the so-called S', being it a region or a neural network. To this end, we here  
82 developed an awake fMRI platform to explore the imprinting network and the long-term  
83 store of imprinting memories in newly-hatched chicks.

84 We exposed (imprinted) chicks on either a preferred (red) or a non-preferred (blue)  
85 colour. After exposure, awake chicks were tested with a sequence alternating the two  
86 colours in the scanner. We could demonstrate that chicks imprinted on red colour showed  
87 activity in pallial and subpallial brain regions involved with storage and memory retrieval,  
88 such as the medial striatum, the arcopallium, the hippocampus, and the nidopallium  
89 caudolaterale (a presumed avian equivalent of mammalian prefrontal cortex).  
90 Surprisingly, chicks imprinted on blue showed little or no activity in the same regions.  
91 However, exploratively we could show that blue-imprinted chicks might have started a  
92 process of secondary imprinting as a result of the exposure to the preferred red colour  
93 inside the scanner. The results indicated an early activation of mesopallium, as well as a  
94 precocial involvement of the *Social Behavior Network* during the first exposure to a  
95 predisposed feature, such as the colour red. We thus, first, established a reliable platform  
96 to investigate the long-term imprinting memory. Second, our results might shed light on  
97 the so-called S', the neural basis of the long-term imprinting memory storage which was  
98 unknown up to now.

## 99 **Results**

100 The present study aimed to better understand the neural networks underlying the different  
101 learning stages of filial imprinting: memory acquisition, long-term memory storage, and  
102 retrieval. To tackle these ambitious questions, we decided to establish a fully non-invasive

103 awake fMRI protocol for newborn chicks. Using the awake fMRI platform, we were able  
104 to capture dynamic neural processes in real-time of imprinting memory at the whole brain  
105 level, allowing us to observe and analyse the intricate interplay of brain regions involved  
106 in filial imprinting memory without interfering with the natural state of the subjects.

## 107 Establishment of a fully non-invasive and awake fMRI for 108 the chicks

109 To enable whole-brain fMRI acquisition in awake chicks, we developed a fully non-  
110 invasive set-up to minimise head and body movements (Figure 1B). Before fMRI scans,  
111 chicks were imprinted for two days on either a preferred red or a non-preferred blue light  
112 ball<sup>20</sup>. Before scanning, chicks were habituated to the scanner noise using a playback of  
113 the magnet noise (Figure 1A). On the third day, after wrapping the animal in a paper  
114 tissue to avoid any body-part movements (such as wings and legs), blocks of plasteline  
115 were used to comfortably fixate the head, minimising movements and scanner's noise by  
116 covering their ears (Figure 1B).

117 To record the spontaneous resting-state (to evaluate the stability and reliability of  
118 the head fixation system) and task-based BOLD signals, a single-shot multi-slice rapid  
119 acquisition with relaxation enhancement (RARE) sequence was adopted from Behroozi  
120 et al <sup>21–23</sup>. Voxel-wise signal-to-noise ratio (SNR) and temporal SNR (tSNR) were  
121 calculated over the resting-state (rs-fMRI) and task-based fMRI (tb-fMRI) scans  
122 respectively. The tSNR of the RARE sequence in each voxel was calculated after  
123 applying motion correction and high-pass temporal filtering (cut-off at 120s) to remove  
124 any linear drift. Temporal SNR in the entire telencephalon ranged from 50 to 100 (Figure

125 S1A, B) for both tb- and rs-fMRI scans. Furthermore, the result indicated highly correlated  
126 SNR and tSNR for both rs- and tb-fMRI scans (Figure S1C, D).

127 In order to verify that adequate fixation was achieved during fMRI scans, we used  
128 the realignment parameters and the results of the frame-wise displacement (FD) to  
129 evaluate the amount of head motion (Figure S2). Overall, the custom-made restrainer  
130 yielded a low level of head movements. There were only 2.02 % (218 volumes) and 1,08%  
131 (19 volumes) of fMRI volumes with FD higher than 0.2 mm (~40% of voxel size) over all  
132 subjects in the task-based and resting-state experiments, respectively (Figure S2A). The  
133 median of frame-wise displacement was ~0.03 mm for both tb-fMRI and rs-fMRI  
134 experiments. However, most head movements occurred in the y-direction (Figure 2B, C).  
135 The respective violin plot information for translations in the y-direction is as follow: tb-  
136 fMRI: max/min = 0.22/-0.31 and median ~ 0; and rs-fMRI: max/min = 0.28/-0.30 and  
137 median ~ 0. The higher motion parameters in the y-direction were most likely due to the  
138 design of the head restrainer, which allowed movements in the dorsoventral direction to  
139 avoid blocking the throat.

140

## 141 Distinct BOLD response to identify the acquisition and 142 long-term storage of imprinting memory

143 We recorded the whole brain BOLD signals from 17 head-restrained awake chicks  
144 already imprinted to either a preferred colour, red (n = 9), or a non-preferred colour, blue  
145 (n = 8). During fMRI scanning, animals were presented with both colours (Figure 1C),  
146 which depending on the previous imprinting training could represent either the imprinted



147 or the control colour. The two colours were presented in a block design manner and a  
148 pseudo-random order (48 trials, 24 per condition, see Methods). For the preferred colour  
149 group, the imprinting colour (Imp) was red and the control (Cont) was blue, while for the  
150 non-preferred colour group the imprinting colour was blue and the control red. To identify  
151 the long-term storage of imprinting memory, we first used the contrast of  $\text{Imp} > \text{Cont}$  by  
152 combining both groups in a conventional generalised linear model (GLM) based statistical  
153 analysis. The first-level results at the single-subject level were then entered into a second-  
154 level analysis (random-effect modelling,  $Z = 2.3$  and  $p < 0.05$  family-wise error (FWE)) to  
155 illustrate the activation clusters at different networks of chick prosencephalon.

156 Before fMRI scans, chicks were exposed to the imprinting stimulus for 2 days, during  
157 which they learned the feature of the imprinting object and stored them as a long-term  
158 memory<sup>1</sup>. Therefore, we expected to find activation in regions involved in memory  
159 retrieval. Surprisingly,  $\text{Red}_{\text{Imp}} + \text{Blue}_{\text{Imp}} > \text{Blue}_{\text{Cont}} + \text{Red}_{\text{Cont}}$  contrast showed no  
160 significantly activated cluster in the chick brain. The activation patterns for both contrasts,  
161  $\text{Red}_{\text{Imp}} + \text{Blue}_{\text{Imp}} > \text{baseline}$  and  $\text{Blue}_{\text{Cont}} + \text{Red}_{\text{Cont}} > \text{baseline}$ , were highly similar (Figure  
162 2A). To get to the bottom of this interference, we examined the interaction between the  
163 group factor and the Red vs. Blue contrast by analysing the following contrasts:  $\text{Red}_{\text{Imp}}$   
164 vs.  $\text{Blue}_{\text{Imp}}$ ,  $\text{Blue}_{\text{Cont}}$  vs.  $\text{Red}_{\text{Cont}}$ ,  $\text{Red}_{\text{Imp}}$  vs.  $\text{Red}_{\text{Cont}}$ , and  $\text{Blue}_{\text{Imp}}$  vs.  $\text{Blue}_{\text{Cont}}$ . As illustrated  
165 in Figures 2B and 2C, robust BOLD activation patterns were found within the  
166 telencephalon for the contrasts:  $\text{Red}_{\text{Imp}} > \text{Blue}_{\text{Imp}}$  and  $\text{Blue}_{\text{Cont}} < \text{Red}_{\text{Cont}}$  contrasts. In  
167 addition, the  $\text{Red}_{\text{Imp}}$  vs.  $\text{Red}_{\text{Cont}}$ , and  $\text{Blue}_{\text{Imp}}$  vs.  $\text{Blue}_{\text{Cont}}$  contrasts demonstrated no  
168 significant differences between the different conditions, same colour serving as the  
169 imprinting or control stimulus.

170 To comprehensively investigate the underlying mechanisms behind this  
171 discrepancy, we conducted a meticulously designed behavioral experiment aimed at  
172 controlling the influence of color on the chick's preferred choice. As represented in Figure  
173 3, we found no significant difference in the colour preference between the two groups  
174 (two-tailed independent sample  $t$ -test:  $t_{(22)}=1.601$ ,  $p=0.124$ ,  $d=0.654$ ; mean  $\pm$  se Red  
175 group:  $0.718 \pm 0.068$ ; Blue group:  $0.558 \pm 0.072$ ). A significant preference for red was  
176 detected in both groups together (two-tailed independent sample  $t$ -test:  $t_{(23)}=2.683$ ,  
177  $p=0.013$ ,  $d=0.548$ ;  $0.638 \pm 0.051$ ). These results confirmed the presence of no significant  
178 differences between the Red and the Blue imprinted groups with regard to the preference  
179 for the red stimulus. These results might support the idea that Blue imprinted chicks  
180 exposed to the preferred colour red immediately started a process of secondary imprinting  
181 toward it inside the scanner.

182 To this end, we decided to analyse both groups independently to determine the brain  
183 activity pattern during the acquisition and the recall phase of a long-term memory of  
184 imprinting. While Imp > Cont contrast in the red group showed robust activation clusters  
185 in many telencephalic as well as diencephalic regions, in the blue group showed no  
186 significant activation clusters.

187 As shown in Figures 2, 3, and S3, this is due to chicks' preference for red over blue  
188 (as demonstrated through the behavioral experiment, ), therefore we used the Cont > Imp  
189 contrast (red > blue colour) during the last 20 minutes of scanning (first 16 trial did not  
190 include in analysis to control the exposure of the animal into the control colour), to  
191 investigate the memory formation phase of a secondary imprinting process<sup>24</sup> elicited by  
192 the presence of the preferred colour red. As illustrated in Figure 4, the voxel-based group

193 analysis showed robust BOLD responses in different visual prosencephalic regions: the  
194 nucleus geniculatus lateralis pars dorsalis (GLd, which receives direct input from the  
195 retina<sup>25</sup>), the right intermediate hyperpallium apicale (IHA, which primarily receives visual  
196 thalamic input<sup>26</sup>), the right hyperpallium intercalatum (HI) and right hyperpallium  
197 densocellulare (HD), and bilaterally the hyperpallium apicale (HA, together with HD  
198 associative hubs of the thalamofugal pathway<sup>26,27</sup>) of the thalamofugal pathway,  
199 bilaterally the nucleus rotundus (Rot, which is the primary thalamic input region of the  
200 tectofugal pathway). Also, parts of the auditory system were activated: bilaterally the  
201 ventromedial part of the Field-L complex and the right nucleus ovoidalis (OV), a thalamic  
202 auditory nucleus receiving direct input from the avian homologue of the inferior colliculus  
203 (*torus semicircularis*<sup>28</sup>) that projects to Field-L. We detected significant activation clusters  
204 in the associative pallial regions nidopallium medial pars medialis (NMm) and bilaterally  
205 in the caudal intermediate medial mesopallium (IMM). Within the two interconnected  
206 *Social Behavior Network* and *Mesolimbic Reward System*, we detected a significant  
207 BOLD increase rightward in the bed nucleus of the stria terminalis (BNST), the nucleus  
208 accumbens (Ac) and the medial striatum (MSt), bilaterally in the septum and leftward in  
209 the posterior pallial amygdala (PoA) and the ventromedial part of hippocampus (Hp-VM).

210 As illustrated in Figures 4 and S4, the voxel-based group analysis during the  
211 imprinting memory retrieval phase in the red group showed robust BOLD responses in  
212 different visual prosencephalic regions: the right GLd, bilaterally in IHA, HI, HD and HA  
213 (Figure 4). We found also a significant BOLD rightward increase in part of the auditory  
214 system, OV.

215 Furthermore, we detected a significant increase in the BOLD signal in the  
216 associative right MNM (IMM + NMm) and nidopallium caudolaterale (NCL) and in left  
217 portions of the caudal mesopallium dorsale (MD) and nidopallium caudocentrale (NCC;  
218 all interconnected regions<sup>31–33</sup>).

219 Within the two interconnected *Social Behavior Network* and *Mesolimbic Reward*  
220 *System*, we detected significant bilateral activation in the ventromedial part of the  
221 hippocampus (Hp-VM), while rightward activation clusters in the bed nucleus of the stria  
222 terminalis (BNST), in the nucleus accumbens (Ac), in the medial striatum (MSt), in the  
223 medial and dorsal arcopallium (respectively AM and AD), in the posterior pallial amygdala  
224 (PoA) and in the preoptic, anterior and ventromedial areas of the hypothalamus  
225 (respectively POA, AH, and VMH).

226

## 227 **Discussion**

228 Imprinting, a well-known form of early learning, has been widely used in the 70's as  
229 a model to study the neurobiology of memory formation (reviews in<sup>10,34</sup>). Evidence for a  
230 crucial role played by the intermediate medial mesopallium (IMM) and NMm (jointly  
231 labelled as MNM) during the acquisition of imprinting memory was obtained. Further  
232 studies showed that the store in the IMM is only temporary, and that a transfer of  
233 information to another, unknown brain region, dubbed S'<sup>35</sup>, occurs after approximately 6  
234 hours. These studies were conducted with either autoradiographic or lesion techniques  
235 and were unable to discover the full imprinting network<sup>36</sup>. To overcome the limitations of  
236 traditional methods, fMRI represents a significant leap forward in our ability to investigate  
237 and comprehend brain activities. By providing an indirect measurement, BOLD, of the

238 whole brain in various circumstances, this cutting-edge technology offers scientists with  
239 a powerful tool for unravelling complex brain networks and sheds light on their roles in  
240 diverse cognitive processes. The enhanced capabilities of fMRI increase our capacity to  
241 investigate the dynamic interplay between different brain areas, allowing us to get a  
242 deeper understanding of the neural processes that underpin cognition and behaviour.

243

244         Here we established a new non-invasive fMRI protocol to study awake brain activity  
245 in newly hatched domestic chicks in order to discover the neural pathways of imprinting  
246 and the identity of S'. After two days of imprinting training, with either a preferred (red) or  
247 a non-preferred (blue) colour, chicks were exposed to a sequence of the two stimulus  
248 colours inside the scanner. Data collected could be informative for a network of brain  
249 regions involved in the acquisition of secondary imprinting memory (blue stimulus), and,  
250 in parallel, a network involved in the long-term storage and retrieval of imprinting memory  
251 (red stimulus).

252         Visual information reaches the pallium both via the tecto- and the thalamofugal visual  
253 pathways. We observed a partial involvement of the nucleus rotundus (Rot), the thalamic  
254 link of the tectofugal pathway during acquisition (Figure 5A). A rotundal involvement had  
255 already been reported in imprinted chicks<sup>37</sup> and together with the present results, it could  
256 suggest a minor tectofugal role during the early stages of imprinting learning. In contrast,  
257 the thalamofugal visual system seems to play a crucial role in processing imprinting  
258 information (as also reviewed in<sup>38</sup>). This pathway consists of the retinorecipient GLd<sup>31</sup> that  
259 projects to the interstitial nucleus of the hyperpallium apicale (IHA) of the visual Wulst,  
260 from where secondary projections reach the three pseudo-layers of the Wulst

261 hyperpallium densocellulare (HD), hyperpallium intercalatum (HI), and hyperpallium  
262 apicale (HA)<sup>39</sup>. We discovered both during memory formation and retrieval (Figure 5B)  
263 significant activity patterns of all these thalamofugal components. Indeed, HD of dark-  
264 reared chicks exhibits topographically organised responses for red and blue objects<sup>40</sup>.  
265 After imprinting on either one of the two colours, such organisation changes along the  
266 rostro-caudal axis showing imprinting-related plasticity already in the Wulst.

267 Previous studies showed that Wulst lesions lead to anterograde amnesia of visual  
268 imprinting memory<sup>40</sup>. This possibly results from the loss of visual projections from HD to  
269 IMM<sup>41,42</sup>, the associative medial pallial area that is crucial for the acquisition of imprinting  
270 memory<sup>10</sup>. IMM projects back to HA, establishing a loop<sup>31</sup>. IMM, the ventrally located  
271 NMm and the nidopallium caudolaterale (NCL) have been shown to be involved during  
272 visual as well as auditory filial imprinting<sup>15,43</sup>. Here we report a significant brain activation  
273 in IMM, NMm, and NCL during memory retrieval and, to a much lesser extent, in IMM and  
274 NMm during memory formation. Indeed, NMm and NCL undergo long-lasting synaptic  
275 changes after multimodal (visuo-auditory) imprinting training<sup>10,43,44</sup>. Imprinting training  
276 also impacts cell proliferation in NMm and NCL, but not in IMM<sup>45</sup>. Thus, these three areas  
277 play important but differential roles in multimodal filial learning and the subsequent  
278 formation of long-term memory. Note that in the present study chicks were also exposed  
279 to the noise produced by the scanner. Thus, NMm and NCL on the one and the auditory  
280 n. ovoidalis (OV) – Field-L pathway on the other side, could conceivably constitute the  
281 neural basis for the acoustic component of acquiring (blue group) or retrieving imprinting  
282 memory (red group).

283           However, the interconnected higher associative regions, NMm and NCL do not only  
284 play a role for long-term memory-related mechanisms<sup>22,44,46,47</sup>. NMm is also involved in  
285 sensorimotor learning and sequential behaviour<sup>48</sup>, while NCL, largely accepted as a  
286 prefrontal-like field<sup>33</sup>, is involved in working memory<sup>49,50</sup>, executive control<sup>51</sup> and in  
287 merging multi-sensory information in long-term memory engrams<sup>52</sup>. This evidence  
288 together with the present findings further supports the involvement of these regions in the  
289 long-term storage and flexible retrieval of a multimodal imprinting memory trace.

290           The motor output component of NMm and NCL is established by their projections to  
291 arcopallium and medial striatum (MSt)<sup>46,53-56</sup>. Possibly, the initially pallially processed  
292 imprinting trace is thereby transferred into a striatum-dependent response strategy. As a  
293 result, striatal S-R associations are formed and once acquired, drive animal's imprinting  
294 behaviour<sup>56</sup>. This also has been shown for passive avoidance learning. Here, the  
295 mnemonic nature of MSt (previously lobus paraolfactorius<sup>12</sup>) goes hand in hand with that  
296 of IMM<sup>34,57,58</sup>, with increased density of synapses and dendritic spines being detectable  
297 some days after training in MSt, but not in IMM<sup>58-60</sup>. Additionally, after imprinting training,  
298 glutamate receptor binding affinity increases both in MSt and arcopallium<sup>61-63</sup>, while, pre-  
299 imprinting arcopallial lesions impair memory acquisition<sup>64</sup>.

300           We found enhanced brain activity in the most medial part of MSt both during  
301 acquisition and retrieval of imprinting memory, while for the dorsal and medial portions of  
302 arcopallium this was only observed for retrieval. These portions of MSt and arcopallium  
303 are enriched in the limbic system-associated membrane protein (LAMP)<sup>65</sup>. We also found  
304 a strong mesolimbic involvement in imprinting memory in the two interconnected *Social*  
305 *Behavior Network* and *Mesolimbic Reward System*<sup>66-68</sup>. Here septum was involved only

306 during memory formation. Arcopallium, preoptic area, anterior and ventromedial  
307 hypothalamus (POA, AH, VMH) were involved only during memory retrieval. In contrast,  
308 Hp, MSt, bed n. of the stria terminalis (BNST), n. accumbens (Ac) and posterior pallial  
309 amygdala (PoA) were involved during both memory formation and retrieval. While  
310 involvement of these systems in social predispositions associated with imprinting had  
311 already been observed<sup>6,69,70</sup>, this is the first evidence for their involvement during  
312 imprinting. Such involvement could represent the motivational component linked to the  
313 association. Indeed, in the context of filial imprinting, emotional-motivational engagement  
314 must be particularly pronounced at different stages of the learning process. The septum  
315 seems to be preferentially involved during the first stages of imprinting and probably  
316 driving the chick's attention toward salient predisposed moving stimuli. Previous studies  
317 also revealed septal involvement during the first exposure to a red object moving with  
318 abrupt changes of speed or an alive conspecific<sup>69,70</sup>. Although BNST, Ac, MSt, and PoA  
319 seem to participate in both imprinting memory formation and retrieval, we found greater  
320 activity in the red group. Such enhanced activity may suggest a stronger emotional-  
321 motivational component after memory consolidation of the imprinting engram.

322       The HD of the Wulst has bidirectional connections with PoA and Hp<sup>71,72</sup>. We found  
323 a hippocampal (Hp) involvement both during imprinting memory formation and retrieval.  
324 The hippocampal formation is known for its role in memory in birds and mammals<sup>73</sup>.  
325 However, *c-fos* immunoreactivity in chicks revealed also a social role of Hp. The dorso-  
326 and ventromedial portions are involved in individual recognition in chicks<sup>74</sup>. The same  
327 portions here were found to be involved in imprinting memory, strengthening a regional  
328 specialisation of hippocampus dedicated to social memory functions. Indeed, Hp projects



329 ipsi- and contralaterally to IMM<sup>59</sup> and is involved in filial imprinting<sup>61</sup>. We found a left Hp  
330 involvement during filial imprinting memory formation (blue group), and a bilateral one  
331 during memory retrieval (red group).

332 Interestingly, the brain activity pattern was predominantly right lateralised. Among  
333 the exceptions was a left Hp involvement during imprinting memory formation (blue  
334 group), and a bilateral Hp involvement during memory retrieval (red group). Lateralisation  
335 is a common feature in the avian brain, especially at different stages of memory  
336 formation<sup>75-77</sup>. Right lateralisation during memory formation has been reported for  
337 passive avoidance learning<sup>78</sup>. Instead, for imprinting learning, time-shifts have been  
338 observed in the lateralisation pattern of IMM. The left IMM is involved at first in learning  
339 the features of the imprinting object, while the right IMM dominates during memory  
340 consolidation and the subsequent establishment of the long-term storage S'<sup>18,79</sup>. A similar  
341 pattern of lateralisation has been proposed in the hemispheric encoding/retrieval  
342 asymmetry model (HERA) in humans, where the left hemisphere plays a dominant role  
343 during memory encoding and the right during retrieval<sup>77</sup>. Such evidence together leads to  
344 the hypothesis of a dual memory system for imprinting, in which different processes -  
345 acquisition and consolidation - take place in different hemispheres, with prominent right  
346 lateralisation for consolidation processes<sup>18</sup>. Indeed, during memory consolidation, a  
347 glutamate injection into the right IMM disrupts imprinting memory, but it does not when  
348 injected into the left hemisphere<sup>80</sup>. Our results may add a novel view on the idea of the  
349 dual memory system: while the visual thalamofugal nucleus GLd was bilaterally activated  
350 during acquisition, only the right side was active during retrieval. It is conceivable that  
351 right hemispheric memory consolidation increased top-down projections onto right sided

352 sensory thalamic nuclei in order to focus attention on learned object properties<sup>81</sup>. This  
353 then could activate and synchronize right hemispheric pallial areas according to  
354 attentional allocation, thereby inducing a right hemispheric superiority in imprinting  
355 memory retrieval<sup>82</sup>.

356 Our findings provide a novel completely non-invasive paradigm for studying neural  
357 mechanisms at birth in newly hatched chicks. Additionally, our data suggests a  
358 prosencephalic neural network that, among others, involves the *Social Behavior Network*,  
359 the *Mesolimbic Reward System*, and the medial meso-/nidopallium for long-term storage  
360 and retrieval of filial imprinting memory. As to be expected, the networks that could be  
361 involved in memory formation and retrieval partially overlapped. However, network activity  
362 was more pronounced and further involved arcopallium and NCL in the retrieval condition.  
363 Thus, consolidation of imprinting memory seems to result in a strengthening and  
364 expansion of the neural system that holds the engram in distributed manner. Within this  
365 perspective, the long-searched site for imprinting memory dubbed as S' by Gabriel Horn  
366 <sup>83</sup> is possibly this whole network within which the "prefrontal" NCL could be a central hub.

## 367 **Acknowledgments**

### 368 **Funding**

369 This work was supported by the MIUR-DAAD Joint Mobility Program (project number  
370 33538), the Deutsche Forschungsgemeinschaft (DFG, German Research Foundation)  
371 through grant SFB 874 (A1, B5) project number 122679504, SFB 1280 (A01, A08, and  
372 F02) project number 316803389. OG was in addition funded by DFG through Gu 227/16-  
373 1 and the European Research Council (ERC) under the European Union's Horizon 2020  
374 research and innovation programme (ERC-2020-ADG, grant agreement No. [101021354,  
375 AVIAN MIND]). GV acknowledges grants from the European Research Council under the  
376 European Union's Seventh Framework Programme (FP7/2007–2013) Grant ERC-2011-  
377 ADG\_20110406, Project no: 461 295517, PREMESOR), by Fondazione Caritro Grant  
378 Bio-marker DSA [40102839], and PRIN 2015. AG acknowledges funding by the European  
379 Research Council (ERC, DISCONN; no. 802371), the Brain and Behavior Foundation  
380 (NARSAD Independent Investigator Grant #25861), the NIH (1R21MH116473-01A1) and  
381 the Telethon foundation (GGP19177).

### 382 **Author Contributions**

383 **Conceptualization:** Onur Güntürkün and Giorgio Vallortigara.

384 **Experiment design:** Mehdi Behroozi, Elena Lorenzi, Onur Güntürkün and Giorgio  
385 Vallortigara.

386 **Data Collection:** Mehdi Behroozi, Elena Lorenzi, and Sepideh Tabrik

387 **Methodology:** Mehdi Behroozi and Sepideh Tabrik

388 **Resources:** Martin Tegenthoff, Alessandro Gozzi, Onur Güntürkün, and Giorgio  
389 Vallortigara

390 **Writing:** All authors

391 **Visualization:** Mehdi Behroozi, Elena Lorenzi, Onur Güntürkün, and Sepideh  
392 Tabrik.

## 393 Competing interests

394 The authors declare no competing interests.

## 395 Data and material availability

396 fMRI data for the chick imprinting and resting-state fMRI are available at  
397 (<https://data.mendeley.com/preview/w6cwvmbxwr>, Will be publicly available after  
398 acceptance). FSL software (<https://fsl.fmrib.ox.ac.uk/fsl/fslwiki/>, version 6.0.4) and  
399 MATLAB (2020b, MathWorks, USA) were used to process fMRI and behavioural data,  
400 respectively. Related processing codes can be found at  
401 <https://github.com/mehdibehroozi/Imprinting-fMRI>. All data needed to evaluate the  
402 conclusions in the paper are present in the paper and/or the Supplementary Materials.

403 A preprint version of the present manuscript is present on bioRxiv (Behroozi, Lorenzi  
404 et al., 2022).

405

406  
407  
408  
409  
410  
411  
412  
413  
414  
415  
416  
417  
418  
419  
420  
421  
422  
423  
424  
425  
426

## References

1. McCabe, B.J. (2013). Imprinting. *Wiley Interdiscip Rev Cogn Sci* 4, 375–390. 10.1002/wcs.1231.
2. Lorenz, K. (1935). Der Kumpan in der Umwelt des Vogels. *Journal für Ornithologie* 1935 83:2 83, 137–213. 10.1007/BF01905355.
3. Spalding, D.A. (1954). Instinct: With original observations on young animals. *The British Journal of Animal Behaviour* 2, 2–11. 10.1016/S0950-5601(54)80075-X.
4. Vallortigara, G. (2021). *Born Knowing: Imprinting and the Origins of Knowledge* (The MIT Press) 10.7551/mitpress/14091.001.0001.
5. Müller-Schwarze, D., and Müller-Schwarze, C. (1971). Olfactory imprinting in a precocial mammal. *Nature* 229, 55–56. 10.1038/229055a0.
6. Lorenzi, E., and Vallortigara, G. (2021). Evolutionary and neural bases of the sense of animacy. In *The Cambridge handbook of animal cognition*, A. B. Kaufman, J. Call, and J. C. Kaufman, eds. (Cambridge University Press).
7. Yamamoto, K., Sun, Z., Hong, B.W., and Reiner, A. (2005). Subpallial amygdala and nucleus taeniae in birds resemble extended amygdala and medial amygdala in mammals in their expression of markers of regional identity. *Brain Res Bull* 66, 341–347. 10.1016/j.brainresbull.2005.02.016.
8. Lemche, E. (2020). Research evidence from studies on filial imprinting, attachment, and early life stress: a new route for scientific integration. *Acta Ethol* 23, 127–133. 10.1007/s10211-020-00346-7.

- 427 9. Vicedo, M. (2013). *The Nature and Nurture of Love* (University of Chicago Press)  
428 10.7208/chicago/9780226020693.001.0001.
- 429 10. Horn, G. (2004). Pathways of the past: The imprint of memory. *Nat Rev Neurosci*  
430 5, 108–120. 10.1038/nrn1324.
- 431 11. Jarvis, E., Güntürkün, O., Bruce, L., Csillag, A., Karten, H., Kuenzel, W., Medina,  
432 L., Paxinos, G., Perkel, D.J., Shimizu, T., et al. (2005). Avian brains and a new  
433 understanding of vertebrate brain evolution. *Nat Rev Neurosci* 6, 151–159.  
434 10.1038/nrn1606.
- 435 12. Reiner, A., Perkel, D.J., Bruce, L.L., Butler, A.B., Csillag, A., Kuenzel, W., Medina,  
436 L., Paxinos, G., Shimizu, T., Striedter, G., et al. (2004). Revised Nomenclature for  
437 Avian Telencephalon and Some Related Brainstem Nuclei. *Journal of*  
438 *Comparative Neurology* 473, 377–414. 10.1002/cne.20118.
- 439 13. Bradley, P., Horn, G., and Bateson, P. (1981). Imprinting - An electron  
440 microscopic study of chick hyperstriatum ventrale. *Exp Brain Res* 41, 115–120.  
441 10.1007/BF00236600.
- 442 14. Horn, G., Bradley, P., and McCabe, B.J. (1985). Changes in the structure of  
443 synapses associated with learning. *Journal of Neuroscience* 5, 3161–3168.  
444 10.1523/jneurosci.05-12-03161.1985.
- 445 15. Bredenkötter, M., and Braun, K. (1997). Changes of neuronal responsiveness in  
446 the mediorostral neo striatum/hyperstriatum after auditory filial imprinting in the  
447 domestic chick. *Neuroscience* 76, 355–365. 10.1016/S0306-4522(96)00381-8.

- 448 16. Bredenkötter, M., and Braun, K. (2000). Development of Neuronal  
449 Responsiveness in the Mediorostral Neostriatum/Hyperstriatum Ventrale during  
450 Auditory Filial Imprinting in Domestic Chicks. *Neurobiol Learn Mem* 73, 114–126.  
451 <https://doi.org/10.1006/nlme.1999.3923>.
- 452 17. Horn, G., McCabe, B.J., and Cipolla-Neto, J. (1983). Imprinting in the domestic  
453 chick: The role of each side of the hyperstriatum ventrale in acquisition and  
454 retention. *Exp Brain Res* 53, 91–98. 10.1007/BF00239401.
- 455 18. Cipolla-Neto, J., Horn, G., and McCabe, B.J. (1982). Hemispheric asymmetry and  
456 imprinting: The effect of sequential lesions to the hyperstriatum ventrale. *Exp*  
457 *Brain Res* 48, 22–27. 10.1007/BF00239569.
- 458 19. Davey, J., McCabe, B., and Horn, G. (1987). Mechanisms of information storage  
459 after imprinting in the domestic chick. *Behavioural Brain Research* 26, 209–210.  
460 10.1016/0166-4328(87)90180-x.
- 461 20. Salzen, E.A., Lily, R.E., and McKeown, J.R. (1971). Colour preference and  
462 imprinting in domestic chicks. *Anim Behav* 19, 542–547. 10.1016/S0003-  
463 3472(71)80109-4.
- 464 21. Behroozi, M., Ströckens, F., Helluy, X., Stacho, M., and Güntürkün, O. (2017).  
465 Functional Connectivity Pattern of the Internal Hippocampal Network in Awake  
466 Pigeons: A Resting-State fMRI Study. *Brain Behav Evol* 90, 62–72.  
467 10.1159/000475591.
- 468 22. Behroozi, M., Helluy, X., Ströckens, F., Gao, M., Pusch, R., Tabrik, S.,  
469 Tegenthoff, M., Otto, T., Axmacher, N., Kumsta, R., et al. (2020). Event-related

- 470 functional MRI of awake behaving pigeons at 7T. *Nat Commun* 11, 1–12.  
471 10.1038/s41467-020-18437-1.
- 472 23. Ungurean, G., Behroozi, M., Böger, L., Helluy, X., Libourel, P.A., Güntürkün, O.,  
473 and Rattenborg, N.C. (2023). Wide-spread brain activation and reduced CSF flow  
474 during avian REM sleep. *Nature Communications* 2023 14:1 14, 1–12.  
475 10.1038/s41467-023-38669-1.
- 476 24. Boakes, R., and Panter, D. (1985). Secondary imprinting in the domestic chick  
477 blocked by previous exposure to a live hen. *Anim Behav* 33, 353–365.  
478 10.1016/S0003-3472(85)80059-2.
- 479 25. Güntürkün, O., and Karten, H.J. (1991). An immunocytochemical analysis of the  
480 lateral geniculate complex in the pigeon (*Columba livia*). *Journal of Comparative*  
481 *Neurology* 314, 721–749. 10.1002/cne.903140407.
- 482 26. Csillag, A., and Montagnese, C.M. (2005). Thalamotelencephalic organization in  
483 birds. In *Brain Research Bulletin (Brain Res Bull)*, pp. 303–310.  
484 10.1016/j.brainresbull.2005.03.020.
- 485 27. Shanahan, M., Bingman, V.P., Shimizu, T., Wild, M., and Güntürkün, O. (2013).  
486 Large-scale network organisation in the avian forebrain: A connectivity matrix and  
487 theoretical analysis. *Front Comput Neurosci* 7. 10.3389/fncom.2013.00089.
- 488 28. Karten, H.J. (1967). The organization of the ascending auditory pathway in the  
489 pigeon (*Columba livia*) I. Diencephalic projections of the inferior colliculus  
490 (nucleus mesencephali lateralis, pars dorsalis). *Brain Res* 6, 409–427.  
491 10.1016/0006-8993(67)90055-8.



- 492 29. Kuenzel, W.J., and Masson, M. (1988). A stereotaxic atlas of the brain of the  
493 chick (*Gallus domesticus*) (Johns Hopkins University Press).
- 494 30. Herold, C., Bingman, V.P., Ströckens, F., Letzner, S., Sauvage, M., Palomero-  
495 Gallagher, N., Zilles, K., and Güntürkün, O. (2014). Distribution of  
496 neurotransmitter receptors and zinc in the pigeon (*Columba livia*) hippocampal  
497 formation: A basis for further comparison with the mammalian hippocampus. *J*  
498 *Comp Neurol* 522, 2553–2575. 10.1002/CNE.23549.
- 499 31. Aoki, N., Yamaguchi, S., Kitajima, T., Takehara, A., Katagiri-Nakagawa, S.,  
500 Matsui, R., Watanabe, D., Matsushima, T., and Homma, K.J. (2015). Critical role  
501 of the neural pathway from the intermediate medial mesopallium to the  
502 intermediate hyperpallium apicale in filial imprinting of domestic chicks (*Gallus*  
503 *gallus domesticus*). *Neuroscience* 308, 115–124.  
504 10.1016/j.neuroscience.2015.09.014.
- 505 32. Atoji, Y., and Wild, J.M. (2009). Afferent and efferent projections of the central  
506 caudal nidopallium in the pigeon (*Columba livia*). *Journal of Comparative*  
507 *Neurology* 517, 350–370. 10.1002/cne.22146.
- 508 33. von Eugen, K., Tabrik, S., Güntürkün, O., and Ströckens, F. (2020). A  
509 comparative analysis of the dopaminergic innervation of the executive caudal  
510 nidopallium in pigeon, chicken, zebra finch, and carrion crow. *Journal of*  
511 *Comparative Neurology*, cne.24878. 10.1002/cne.24878.
- 512 34. Rose, S.P.R. (2000). God's organism? The chick as a model system for memory  
513 studies. *Learning and Memory* 7, 1–17. 10.1101/lm.7.1.1.

- 514 35. Honey, R.C., Horn, G., Bateson, P., and Walpole, M. (1995). Functionally Distinct  
515 Memories for Imprinting Stimuli: Behavioral and Neural Dissociations. *Behavioral*  
516 *Neuroscience* 109, 689–698. 10.1037/0735-7044.109.4.689.
- 517 36. Horn, G., McCabe, B.J., and Bateson, P.P.G. (1979). An autoradiographic study  
518 of the chick brain after imprinting. *Brain Res* 168, 361–373. 10.1016/0006-  
519 8993(79)90176-8.
- 520 37. Harvey, R.J., McCabe, B.J., Solomon, R.O., Horn, G., and Darlison, M.G.  
521 (1998). Expression of the GABAA receptor  $\gamma 4$ -subunit gene: Anatomical  
522 distribution of the corresponding mRNA in the domestic chick forebrain and the  
523 effect of imprinting training. *European Journal of Neuroscience* 10, 3024–3028.  
524 10.1111/j.1460-9568.1998.00354.x.
- 525 38. Nakamori, T., Maekawa, F., Sato, K., Tanaka, K., and Ohki-Hamazaki, H. (2013).  
526 Neural basis of imprinting behavior in chicks. *Dev Growth Differ* 55, 198–206.  
527 10.1111/dgd.12028.
- 528 39. Stacho, M., Herold, C., Rook, N., Wagner, H., Axer, M., Amunts, K., and  
529 Güntürkün, O. (2020). A cortex-like canonical circuit in the avian forebrain.  
530 *Science* (1979) 369. 10.1126/science.abc5534.
- 531 40. Maekawa, F., Komine, O., Sato, K., Kanamatsu, T., Uchimura, M., Tanaka, K.,  
532 and Ohki-Hamazaki, H. (2006). Imprinting modulates processing of visual  
533 information in the visual wulst of chicks. *BMC Neuroscience* 2006 7:1 7, 1–13.  
534 10.1186/1471-2202-7-75.

- 535 41. Shimizu, T., Cox, K., and Karten, H.J. (1995). Intratelencephalic projections of the  
536 visual wulst in pigeons (*Columba livia*). *Journal of Comparative Neurology* 359,  
537 551–572. 10.1002/cne.903590404.
- 538 42. Nakamori, T., Sato, K., Atoji, Y., Kanamatsu, T., Tanaka, K., and Ohki-Hamazaki,  
539 H. (2010). Demonstration of a neural circuit critical for imprinting behavior in  
540 chicks. *Journal of Neuroscience* 30, 4467–4480. 10.1523/JNEUROSCI.3532-  
541 09.2010.
- 542 43. Bock, J., Schnabel, R., and Braun, K. (1997). Role of the dorso - caudal  
543 neostriatum in filial imprinting of the domestic chick: A pharmacological and  
544 autoradiographical approach focused on the involvement of NMDA-receptors.  
545 *European Journal of Neuroscience* 9, 1262–1272. 10.1111/j.1460-  
546 9568.1997.tb01481.x.
- 547 44. Metzger, M., Jiang, S., and Braun, K. (1998). Organization of the dorsocaudal  
548 neostriatal complex: A retrograde and anterograde tracing study in the domestic  
549 chick with special emphasis on pathways relevant to imprinting. *Journal of*  
550 *Comparative Neurology* 395, 380–404. 10.1002/(SICI)1096-  
551 9861(19980808)395:3<380::AID-CNE8>3.0.CO;2-Z.
- 552 45. Komissarova, N. V., and Anokhin, K. V. (2008). Effects of an imprinting procedure  
553 on cell proliferation in the chick brain. *Neurosci Behav Physiol* 38, 289–296.  
554 10.1007/s11055-008-0041-z.

- 555 46. Atoji, Y., and Wild, J.M. (2012). Afferent and efferent projections of the  
556 mesopallium in the pigeon (*Columba livia*). *Journal of Comparative Neurology*  
557 *520*, 717–741. 10.1002/cne.22763.
- 558 47. Rook, N., Tuff, J.M., Isparta, S., Masseck, O.A., Herlitze, S., Güntürkün, O., and  
559 Pusch, R. (2021). AAV1 is the optimal viral vector for optogenetic experiments in  
560 pigeons (*Columba livia*). *Commun Biol* *4*, 1–16. 10.1038/s42003-020-01595-9.
- 561 48. Helduser, S., and Güntürkün, O. (2012). Neural substrates for serial reaction time  
562 tasks in pigeons. *Behavioural Brain Research* *230*, 132–143.  
563 10.1016/j.bbr.2012.02.013.
- 564 49. Diekamp, B., Kalt, T., and Güntürkün, O. (2002). Working memory neurons in  
565 pigeons. *J Neurosci* *22*, RC210–RC210. 10.1523/jneurosci.22-04-j0002.2002.
- 566 50. Veit, L., Hartmann, K., and Nieder, A. (2014). Neuronal correlates of visual  
567 working memory in the corvid endbrain. *Journal of Neuroscience* *34*, 7778–7786.  
568 10.1523/JNEUROSCI.0612-14.2014.
- 569 51. Rose, J., and Colombo, M. (2005). Neural correlates of executive control in the  
570 avian brain. *PLoS Biol* *3*, 1139–1146. 10.1371/journal.pbio.0030190.
- 571 52. Moll, F.W., and Nieder, A. (2015). Cross-modal associative mnemonic signals in  
572 crow endbrain neurons. *Current Biology* *25*, 2196–2201.  
573 10.1016/j.cub.2015.07.013.
- 574 53. Kröner, S., and Güntürkün, O. (1999). Afferent and efferent connections of the  
575 caudolateral neostriatum in the pigeon (*Columba uvia*): A retro- and anterograde

- 576 pathway tracing study. *Journal of Comparative Neurology* 407, 228–260.  
577 10.1002/(SICI)1096-9861(19990503)407:2<228::AID-CNE6>3.0.CO;2-2.
- 578 54. Schnabel, R., Metzger, M., Jiang, S., Hemmings, H.C., Greengard, P., and Braun,  
579 K. (1997). Localization of dopamine D1 receptors and dopaminoceptive neurons  
580 in the chick forebrain. *Journal of Comparative Neurology* 388, 146–168.  
581 10.1002/(SICI)1096-9861(19971110)388:1<146::AID-CNE10>3.0.CO;2-T.
- 582 55. Metzger, M., Jiang, S., and Braun, K. (2002). A quantitative immuno-electron  
583 microscopic study of dopamine terminals in forebrain regions of the domestic  
584 chick involved in filial imprinting. *Neuroscience* 111, 611–623. 10.1016/S0306-  
585 4522(01)00611-X.
- 586 56. Csillag, A. (1999). Striato-telencephalic and striato-tegmental circuits: Relevance  
587 to learning in domestic chicks. *Behavioural Brain Research* 98, 227–236.  
588 10.1016/S0166-4328(98)00088-6.
- 589 57. Gibbs, M.E. (2008). Memory systems in the chick: Regional and temporal control  
590 by noradrenaline. *Brain Res Bull* 76, 170–182.  
591 10.1016/j.brainresbull.2008.02.021.
- 592 58. Sojka, M., Davies, H.A., Harrison, E., and Stewart, M.G. (1995). Long-term  
593 increases in synaptic density in chick CNS after passive avoidance training are  
594 blocked by an inhibitor of protein synthesis. *Brain Res* 684, 209–214.  
595 10.1016/0006-8993(95)00403-D.

- 596 59. Bradley, P., Davies, D.C., and Horn, G. (1985). Connections of the hyperstriatum  
597 ventrale of the domestic chick (*Gallus domesticus*). *Journal of anatomy (Print)*  
598 *140*, 577–589.
- 599 60. Stewart, M.G., and Rusakov, D.A. (1995). Morphological changes associated with  
600 stages of memory formation in the chick following passive avoidance training.  
601 *Behavioural Brain Research* *66*, 21–28. 10.1016/0166-4328(94)00119-Z.
- 602 61. McCabe, B.J., and Horn, G. (1994). Learning-related changes in Fos-like  
603 immunoreactivity in the chick forebrain after imprinting. *Proc Natl Acad Sci U S A*  
604 *91*, 11417–11421. 10.1073/pnas.91.24.11417.
- 605 62. Johnston, A.N., Rogers, L.J., and Johnston, G.A.R. (1993). Glutamate and  
606 imprinting memory: the role of glutamate receptors in the encoding of imprinting  
607 memory. *Behavioural Brain Research* *54*, 137–143. 10.1016/0166-  
608 4328(93)90072-X.
- 609 63. Izawa, E.I., Yanagihara, S., Atsumi, T., and Matsushima, T. (2001). The role of  
610 basal ganglia in reinforcement learning and imprinting in domestic chicks.  
611 *Neuroreport* *12*, 1743–1747. 10.1097/00001756-200106130-00045.
- 612 64. Lowndes, M., Davies, D.C., and Johnson, M.H. (1994). Archistriatal Lesions  
613 Impair the Acquisition of Filial Preferences During Imprinting in the Domestic  
614 Chick. *European Journal of Neuroscience* *6*, 1143–1148. 10.1111/j.1460-  
615 9568.1994.tb00612.x.

- 616 65. Yamamoto, K., and Reiner, A. (2005). Distribution of the limbic system-associated  
617 membrane protein (LAMP) in pigeon forebrain and midbrain. *Journal of*  
618 *Comparative Neurology* 486, 221–242. 10.1002/cne.20562.
- 619 66. Newman, S.W. (1999). The medial extended amygdala in male reproductive  
620 behavior. A node in the mammalian social behavior network. *Ann N Y Acad Sci*  
621 877, 242–257. 10.1111/j.1749-6632.1999.tb09271.x.
- 622 67. O'Connell, L.A., and Hofmann, H.A. (2011). The Vertebrate mesolimbic reward  
623 system and social behavior network: A comparative synthesis. *Journal of*  
624 *Comparative Neurology* 519, 3599–3639. 10.1002/cne.22735.
- 625 68. Goodson, J.L., and Kingsbury, M.A. (2013). What's in a name? Considerations of  
626 homologies and nomenclature for vertebrate social behavior networks. *Horm*  
627 *Behav* 64, 103–112. 10.1016/j.yhbeh.2013.05.006.
- 628 69. Lorenzi, E., Mayer, U., Rosa-Salva, O., and Vallortigara, G. (2017). Dynamic  
629 features of animate motion activate septal and preoptic areas in visually naïve  
630 chicks (*Gallus gallus*). *Neuroscience* 354, 54–68.  
631 10.1016/j.neuroscience.2017.04.022.
- 632 70. Mayer, U., Rosa-Salva, O., and Vallortigara, G. (2017). First exposure to an alive  
633 conspecific activates septal and amygdaloid nuclei in visually-naïve domestic  
634 chicks (*Gallus gallus*). *Behavioural Brain Research* 317, 71–81.  
635 10.1016/j.bbr.2016.09.031.

- 636 71. Atoji, Y., Sarkar, S., and Wild, J.M. (2018). Differential projections of the  
637 densocellular and intermediate parts of the hyperpallium in the pigeon (*Columba*  
638 *livia*). *Journal of Comparative Neurology* 526, 146–165. 10.1002/cne.24328.
- 639 72. Atoji, Y., Saito, S., and Wild, J.M. (2006). Fiber connections of the compact  
640 division of the posterior pallial amygdala and lateral part of the bed nucleus of the  
641 stria terminalis in the pigeon (*Columba livia*). *Journal of Comparative Neurology*  
642 499, 161–182. 10.1002/cne.21042.
- 643 73. Colombo, M., and Broadbent, N. (2000). Is the avian hippocampus a functional  
644 homologue of the mammalian hippocampus? *Neurosci Biobehav Rev* 24, 465–  
645 484. 10.1016/S0149-7634(00)00016-6.
- 646 74. Corrales Parada, C.D., Morandi-Raikova, A., Rosa-Salva, O., and Mayer, U.  
647 (2021). Neural basis of unfamiliar conspecific recognition in domestic chicks  
648 (*Gallus Gallus domesticus*). *Behavioural Brain Research* 397, 112927.  
649 10.1016/j.bbr.2020.112927.
- 650 75. Moorman, S., and Nicol, A.U. (2015). Memory-related brain lateralisation in birds  
651 and humans. *Neurosci Biobehav Rev* 50, 86–102.  
652 10.1016/j.neubiorev.2014.07.006.
- 653 76. Rogers, L.J., Vallortigara, G., and Andrew, R.J. (2013). *Divided brains: The*  
654 *biology and behaviour of brain asymmetries* (Cambridge University Press)  
655 10.1017/CBO9780511793899.
- 656 77. Tulving, E., Kapur, S., Craik, F.I.M., Moscovitch, M., and Houle, S. (1994).  
657 Hemispheric encoding/retrieval asymmetry in episodic memory: Positron emission



658 tomography findings. *Proc Natl Acad Sci U S A* 91, 2016–2020.  
659 10.1073/pnas.91.6.2016.

660 78. Lössner, B., and Rose, S.P.R. (1983). Passive Avoidance Training Increases  
661 Fucokinase Activity in Right Forebrain Base of Day-Old Chicks. *J Neurochem* 41,  
662 1357–1363. 10.1111/j.1471-4159.1983.tb00833.x.

663 79. McCabe, B.J. (1991). Hemispheric asymmetry of learning-induced changes. In  
664 *Neural and Behavioural Plasticity* (Oxford University Press), pp. 262–276.  
665 10.1093/acprof:oso/9780198521846.003.0010.

666 80. Johnston, A.N.B., and Rogers, L.J. (1998). Right hemisphere involvement in  
667 imprinting memory revealed by glutamate treatment. *Pharmacol Biochem Behav*  
668 60, 863–871. 10.1016/S0091-3057(98)00073-2.

669 81. Kastner, S., and Ungerleider, L.G. (2000). Mechanisms of visual attention in the  
670 human cortex. *Annu Rev Neurosci* 23, 315–341.  
671 10.1146/annurev.neuro.23.1.315.

672 82. Saalman, Y.B., Pinsk, M.A., Wang, L., Li, X., and Kastner, S. (2012). The  
673 pulvinar regulates information transmission between cortical areas based on  
674 attention demands. *Science* (1979) 337, 753–756. 10.1126/science.1223082.

675 83. Horn, G. (1985). Memory, imprinting, and the brain : an inquiry into mechanisms.  
676 10, 315.

677

678



## 680 Figures

681 **Figure 1-** Experimental setups and stimulation sequence for awake chick fMRI. (A) Imprinting  
682 cage. Newborn chicks were first exposed to a hollow plastic ball with a flickering red/blue light at  
683 a frequency of 5Hz. (B) Custom-made restrainer and 7T fMRI system. Awake chicks were placed  
684 in an MR-compatible tube. To immobilise non-invasively the animals, a beak holder was used to  
685 control the beak movements, and blocks of plastelins were used to cover the ears and reduce  
686 head movements. To avoid body-part movements, animals were wrapped in paper tissue before  
687 fixating the head. Subsequently, the animal's body was taped to the restrainer. (C) A sequence  
688 of the block design experiment paradigm. Visual stimuli were presented in blocks of 16 s followed  
689 by 24 s dark. During the ON blocks, the visual stimulus (red/blue light) flickered at a frequency of  
690 5Hz.

691 **Figure 2-** Colour preference of different groups. (A) GLM analysis was used to demonstrate  
692 activated networks during imprinting and control trials by examining RedImp + BlueImp > baseline  
693 (red map) and BlueCont + RedCont > baseline (blue map) contrasts. The colour maps show the  
694 activation significance of group-averaged data from 17 chicks (9 red group + 8 blue group) in the  
695 axial view (group analysis using a mixed model FLAME 1+2 method,  $Z = 2.3$ , and  $p < 0.05$  FEW  
696 corrected at the cluster level). (B) the contrast map shows the significant increase of BOLD signal  
697 during Red colour as imprinting stimulus compared to Blue colour as imprinting stimulus (RedImp  
698 > BlueImp contrast, 9 chicks for red group and 8 chicks for blue group). (C) Activation map  
699 showing the strong BOLD response during the Red colour as control stimulus for the blue group  
700 compared to the Blue colour as control stimulus for red group (BlueCont < RedCont, 9 chicks for  
701 red group and 8 chicks for blue group). The functional maps were superimposed on the high-  
702 resolution anatomical data at the different levels of an ex vivo chick brain (in greyscale).

703 **Figure 3 –** Colour preference after imprinting. The boxplot in grey represents the colour  
704 preference in both red and blue imprinted groups together. The asterisk represents a significant  
705 difference from chance (dotted line). To best represent the data, we provided each subject  
706 preference (red points are Red imprinted chicks and blue points are Blue imprinted chicks) and a  
707 violin plot for each imprinting group (blue and red respectively) representing the group distribution.  
708 No significant difference was detected between the two groups in the colour preference.

709 **Figure 4-** BOLD response pattern during the acquisition of imprinting memory. Statistical maps  
710 for the BOLD signal increase in the contrast of red light versus blue light in the Blue group ( $n = 8$ ,  
711  $Z = 2.3$ , and  $p < 0.05$  FEW corrected at the cluster level). The top row images show the 3D  
712 representation of the activation pattern inside a translucent chick brain. A 3D depiction of the  
713 chick brain is represented at the bottom of the left column with an example window at the level of  
714 A 7.0. Anatomical borders (black lines) are based on the contrast difference of ex-vivo chick brain  
715 and Chick atlas<sup>29,30</sup>. The corresponding abbreviations of ROIs are listed in the Table S1.

716 **Figure 5-** BOLD response pattern during imprinting memory retrieval. The high-resolution coronal  
717 slices at the different levels of an ex-vivo chick brain are in greyscale, while the contrast map  
718 represents the activation pattern during the presentation of the preferred imprinting object after  
719 imprinting learning has already occurred (Red group, the contrast of red light versus blue light  
720 conditions,  $n = 9$ ,  $Z = 3.1$  and  $p < 0.05$  FEW corrected at the cluster level). The top row images

721 show the 3D representation of the activation pattern inside a translucent chick brain. A 3D  
722 depiction of the chick brain is represented bottom left with an example window at the level of A  
723 7.4. Anatomical borders (black lines) are based on the contrast difference of ex-vivo chick brain  
724 and Chick atlas <sup>29,30</sup>. The corresponding abbreviations of ROIs are listed in Table S1.

725 **Figure 6-** Schematic depiction of the activated prosencephalic areas during different phases of  
726 imprinting memory. (A) Network activated during imprinting memory acquisition are represented  
727 in colourful circles. (B) Network activated during imprinting memory retrieval are represented in  
728 colourful circles. The grey circles represent no activation. The corresponding abbreviations of  
729 ROIs are listed in the Table S1.

730

731

## 732 **Material and Methods**

### 733 **Subjects**

734 All procedures here presented followed all the applicable European Union and Italian  
735 laws, and guidelines for animals' care and use and were approved by the Ethical  
736 Committee of the University of Trento OPBA and by the Italian Health Ministry (permit  
737 number 738/2019). Fifty females were used in the present study. Twenty-six for the MRI  
738 procedure: red group (n = 9) imprinted to red colour, blue group (n = 8) imprinted to blue  
739 colour, and resting-state group (n= 9). Twenty-four for the behavioural experiment: red  
740 group (n = 12) imprinted to the red colour, blue group (n = 12) imprinted to the blue colour.  
741 Each chick underwent the experimental procedure only once.

742 A local commercial hatchery (Azienda Agricola Crescenti, Brescia, Italy) provided  
743 fertilised eggs of the Aviagen Ross 308 strain (*Gallus gallus domesticus*). Eggs were  
744 incubated and hatched in the laboratory under controlled temperature (37.7°C) and  
745 humidity (60%) in darkness using FIEM MG140/200 Rural LCD EVO incubators. Soon  
746 after hatching, chicks were sexed by feather dimorphism, with a black cap on the head in  
747 order to prevent any visual stimulation. Twenty-six females were used in the present  
748 study. Females were used because they are known to exhibit stronger filial attachment  
749 with the imprinting object (Cailotto et al., 1989; Vallortigara, 1992; Vallortigara et al.,  
750 1990). Each chick underwent the experimental procedure only once. At the end of the  
751 experimental procedure, on post-hatching day 3, chicks were caged in groups with water  
752 and food *ad libitum*, at constant temperature (32.3°C) and with a 12:12 day-night light  
753 cycle until they were donated to local farmers.

## 754        **Imprinting**

755            On the day of hatching, chicks were caged individually at a constant temperature of  
756 32.3°C with water and food. In each cage (28x40x32 cm) the imprinting stimulus, a hollow  
757 plastic ball (diameter 3.5 cm), was suspended in the middle (7 cm from the floor, Figure  
758 1 A). Two optical fibres (diameter of 2mm) inserted in the ball were flickering at 5 Hz.  
759 Chicks prefer to imprint on a flickering than on a stationary light (James, 1959). For one  
760 group of chicks, the ball was flickering with red light (N = 9, dominant wavelength = 642  
761 nm, intensity = 16.45 cd/m<sup>2</sup>), for the other group with blue light (N = 8, dominant  
762 wavelength = 465 nm, intensity = 16.45 cd/m<sup>2</sup>). Being the only light provided in the  
763 environment, the established setup by Behroozi et al. (Behroozi et al., 2020) and a  
764 custom-written MATLAB code were used to automatically switch on and off the light,  
765 following a day-night cycle 12:12. During the daytime, to habituate the subjects to the  
766 noise of the scanner, a recording of the sound was provided twice per day, for a total  
767 amount of 5 hours per day, by two loudspeakers (Logitech) placed outside the cages.

768

## 769        **Acquisition and Pre-processing of fMRI data**

770            All MRI experiments were recorded using a horizontal-bore small animal MRI  
771 scanner (7.0 T Bruker BioSpin, Ettlingen, Germany) equipped with a BGA-9 gradient set  
772 (380 mT/m, max. linear slew rate 3,420 T/m/s). A 72 mm transmit birdcage resonator was  
773 used for radio-frequency transmission. To reduce the motion artifacts resulting from body  
774 parts' movements, a single-loop 20 mm surface coil was placed around the chicks' head  
775 for signal reception.

776       **Localiser.** At the beginning of each scanning session, a set of scout images  
777 (coronal, horizontal, and sagittal scans) were recorded as localisers to identify the position  
778 and orientation of the chick's brain inside the MRI machine. The scout images were  
779 acquired using a multi-slice rapid acquisition (RARE) sequence with the following  
780 parameters: repetition time (TR) = 3000 ms, effective echo time ( $TE_{eff}$ ) = 41.2 ms, RARE  
781 factor = 32,  $N_{average} = 2$ , acquisition matrix =  $128 \times 128$ , the field of view  
782 (FoV) =  $20 \times 20$  mm, spatial resolution =  $0.156 \times 0.156$  mm<sup>2</sup>, slice thickness = 1 mm,  
783 number of slices = 8, slice orientation = coronal/horizontal/sagittal, with a total scan time  
784 of 18 s. This information has been used to position 9 coronal slices in a way ( $\sim 40^\circ$   
785 regarding coronal direction) to cover the entire telencephalon to record the fMRI time  
786 series.

787       **fMRI (task).** The blood-oxygen-level-dependent (BOLD) time series were recorded  
788 using a single-shot multi-slice RARE sequence adopted from Behroozi et al. (Behroozi et  
789 al., 2020, 2018) with the following parameters: TR/ $TE_{eff}$  = 4000/51.04 ms, RARE factor =  
790 42, acquisition matrix =  $64 \times 64$ , FoV =  $30 \times 30$  mm<sup>2</sup>, 9 coronal slices no gap between  
791 slices, slice thickness = 1 mm, slice order = interleaved. Since the eyes' size is  
792 comparable to brain's one, two saturation slices were manually positioned on the eyes to  
793 saturate the possible eye movement artifacts, which can corrupt the BOLD signal. A total  
794 of 540 volumes were recorded for each animal.

795       **fMRI (Rest).** Whole-brain resting-state fMRI data (200 volumes) of nine chicks were  
796 recorded using a single-shot RARE sequence with the same parameter as the task fMRI  
797 sequence.

798       **Structural MRI.** High-resolution anatomical images were acquired using a RARE  
799 sequence with following parameters: TR/TE<sub>eff</sub> = 6000/42.04 ms, RARE factor = 16,  
800 N\_Average = 4, acquisition matrix = 160 × 160, FoV = 30 × 30 mm<sup>2</sup>, 39 coronal slices  
801 with no gap between slices, slice thickness = 0.33 mm, total scan time = 4 min.

802       **Experimental Task.** Inside the fMRI machine, chicks were presented with two  
803 different stimulus types, imprinted (red/blue) and control colour (blue/red) with the same  
804 wavelength and intensity as the training phase. The light stimuli were generated using the  
805 established setup by Behroozi et al. (Behroozi et al., 2020). Stimuli were presented in a  
806 pseudo-random order in an ON/OFF block design experiment (maximum two trials in a  
807 row were of the same colour). The duration of ON blocks was 16 s. ON blocks were  
808 interleaved with a rest period of 24 s (OFF blocks, inter-trial interval (ITI)). In total, 48 trials  
809 were recorded during an fMRI session from each animal (24 trials per stimulus).

810       **Apparatus.** A critical issue during awake fMRI scanning of animals is motion  
811 artifacts. Therefore, immobilisation of the animal's head is essential to acquire an  
812 accurate fMRI time series. To this end, awake chicks were immobilised in a nonmagnetic  
813 custom-made restrainer, composed of a beak holder, blocks of plasticine around the head  
814 to immobilise it in a comfortable way, and a round RF coil on top of the head (Figure 1B).  
815 Before the head fixation, the animal's body was wrapped in paper tissue to prevent the  
816 other body parts' movement (such as wings and feet) to avoid any possible motion  
817 artifacts. The animal's body inside the paper tissue was tapped to the main body of the  
818 restrainer using a piece of medical tape.

819       **fMRI data processing**



820 All BOLD time series were pre-processed using the FMRIB Software Library (FSL,  
821 version 6.0.4, <https://fsl.fmrib.ox.ac.uk/fsl/fslwiki>), the Analysis of Functional  
822 NeuroImages (AFNI, version 20.0.09 <https://afni.nimh.nih.gov/>), and Advanced  
823 Normalization Tools (ANTs, <http://stnava.github.io/ANTs/>) software. We performed the  
824 following pre-processing steps for each run: (i) converting dicom files to nifti format (using  
825 dcm2niix function); (ii) upscaling the voxel size by a factor of 10 (using AFNI's 3drefit);  
826 (iii) discarding the first 5 volumes to ensure longitudinal magnetization reached steady  
827 state; (iv) motion correction using MCFLIRT (which aligns each volume to the middle  
828 volume of each run); (v) slice time correction to account for the long whole-brain  
829 acquisition time (4000 ms); interleaved acquisitions); (vi) despiking using 3dDespike  
830 algorithm in AFNI; (vii) removing non-brain tissue (using BET and manual cleaning); (viii)  
831 spatial smoothing with FWHM = 8 mm (using FSL's SUSAN, after upscaling voxel size  
832 by factor of 10); (ix) global intensity normalization with grand mean = 10000 across  
833 scanning sessions for group analysis; (x) high-pass temporal filtering to remove slow drifts  
834 (cut-off at 100s); (xi) anatomical brain extraction (using BET function and cleaned  
835 manually); (xii) registration of the functional data to the high-resolution structural images  
836 using affine linear registration (FLIRT function, six degrees of freedom). For spatial  
837 normalization, a population-based template was constructed using  
838 antsMultivariateTemplateConstruction.sh script (ANTs). FMRIB's Nonlinear Image  
839 Registration Tool (FNIRT) (Andersson et al., 2007) was used to spatially normalize the  
840 single subject anatomical images to the population-based template as a standard space.  
841 The head motion of animals was quantified using framewise displacement (FD) (Power  
842 et al., 2014). Three animals' data were excluded due to the excessive head motion (over

843 20% of volumes were contaminated with  $FD > 0.2\text{mm}$ ). For the remaining animals, the  
844 detected motion outliers were modeled as confound regressors during the general linear  
845 model (GLM) analysis to reduce the impact of head motion.

## 846 General linear model (GLM) analysis

847 Whole-brain statistical analysis was performed using the FEAT (FMRI Expert  
848 Analysis Tool) to assess stimulus-evoked activation patterns. Single-subject GLM  
849 analysis was carried out to convolve the established double-gamma avian hemodynamic  
850 response function in pigeon brain by Behroozi et al. (Behroozi et al., 2020) (the closest  
851 brain in the structural organization to the chick brain) to the explanatory variables (on/off  
852 stimulation). In the first GLM, we incorporated the complete fMRI timeseries using the  
853 following two explanatory variables (EVs) and their temporal derivatives: (i) imprinting  
854 trials (indicated by red/blue, 24 trials) and (ii) control trials (indicated by blue/red, 24 trials).  
855 In the second GLM, we employed three EVs and their temporal derivatives: (i) imprinting  
856 trials (last 16 trials); (ii) control trials (last 16 trials); (iii) junk trials (the first 16 trials  
857 comprising 8 imprinting and 8 control trials, were used as habituation period to the real  
858 magnet environment). In addition, six estimated head motion parameters (three  
859 translations and three rotations) and outlier volumes detected based on the FD analysis  
860 were modelled as confound EVs to remove the residual motion artifacts. To perform  
861 group inference, subject-level parameter estimates were taken into the second-level  
862 analysis using the mixed-effect model (FLAME1+2) to produce group-level estimates of  
863 each condition. FLAME 1+2 cluster-based approach has been used to threshold the  
864 group-level statistical maps for contrasts of interest with a cluster defining voxel threshold  
865 of  $p < 0.001$  ( $Z > 3.1$ ) for red group and  $p < 0.01$  ( $Z > 2.3$ ) for blue group and entire

866 timeseries analysis and Family Error Wise (FEW) cluster significance threshold of  $p =$   
867 0.05.

## 868 Visualization

869 To visualize the results, we took advantage of the high-resolution anatomical image  
870 acquired for another study. Briefly, five post-mortem chick brains were scanned using a  
871 fast-low angle shot (FLASH) sequence with following parameters: TR/TE = 50/4 ms,  
872 N\_average = 6, acquisition matrix = 400 × 400 × 500, voxels size = 0.05 × 0.05 × 0.05  
873 mm<sup>3</sup>, total scan time = 19 h 48 min. The population-based template was co-registered  
874 nonlinearly (using FNIRT) to the high-resolution anatomical image of the chick brain. The  
875 contrasts of interest, eventually, were non-linearly warped to the high-resolution  
876 anatomical image. MANGO software (<http://ric.uthscsa.edu/mango/mango.html>, version  
877 4.1) was used for 3D visualization of the activation patterns. Surf Ice software  
878 (<https://www.nitrc.org/projects/surfice/>, version v1.0.20201102 64bit x86-64 Windows)  
879 was used for surface rendering the chick brains with overlays to illustrate activated  
880 networks during imprinting acquisition and retrieval memory.

## 881 Behavioural experiment

882 Similar to the imprinting procedure employed for the MRI experiment, chicks were  
883 individually caged on the day of hatching with the imprinting object until day 3. The Red  
884 imprinted group was exposed for two days to the red flickering light (N =12), while the  
885 Blue imprinted group to the blue flickering light (N = 12).

886 On day 3 all chicks were individually exposed to the pseudo random sequence of  
887 red and blue colours that was employed for the stimulation inside the scanner (for details

888 see section Acquisition and Pre-processing of fMRI data - Experimental task). Each chick  
889 saw 24 times its imprinting colour (red/blue) and 24 times the control colour (red/blue).

890 After the exposure, each chick was tested individually inside a running wheel to  
891 evaluate its colour preference. The test in the running wheel lasted a total of 10 minutes.  
892 Each colour was presented for 5 minutes. The sequence of colour presentation was  
893 counterbalanced between subjects.

894 The dependent variable measured was the distance (cm) covered by each subject  
895 toward the red and the blue. To estimate chicks' colour preference, we calculated an  
896 index using the formula:

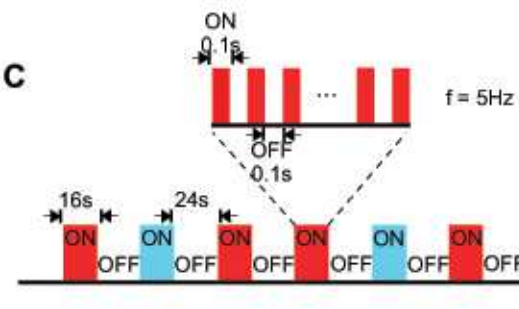
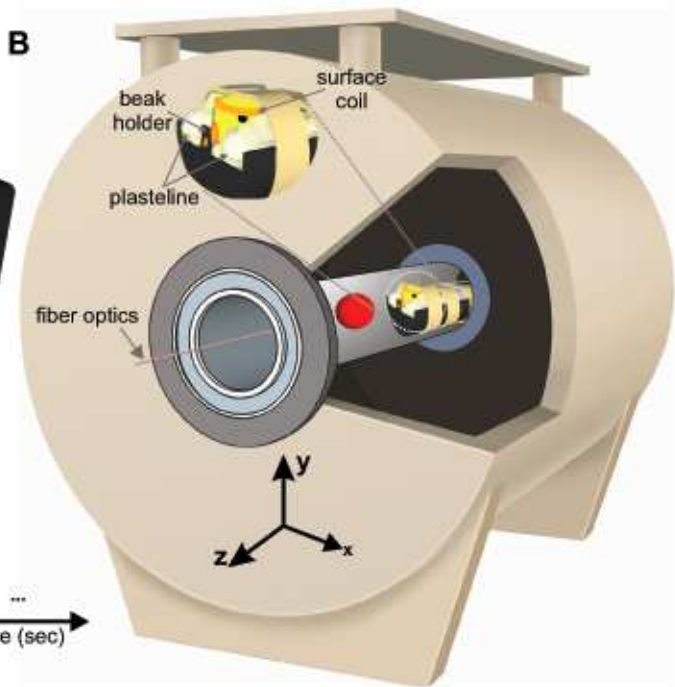
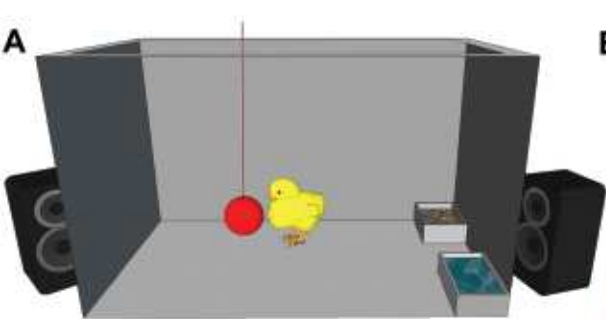
$$897 \quad \text{Colour preference} = \frac{\text{cm toward red}}{\text{cm toward red} + \text{cm toward blue}}$$

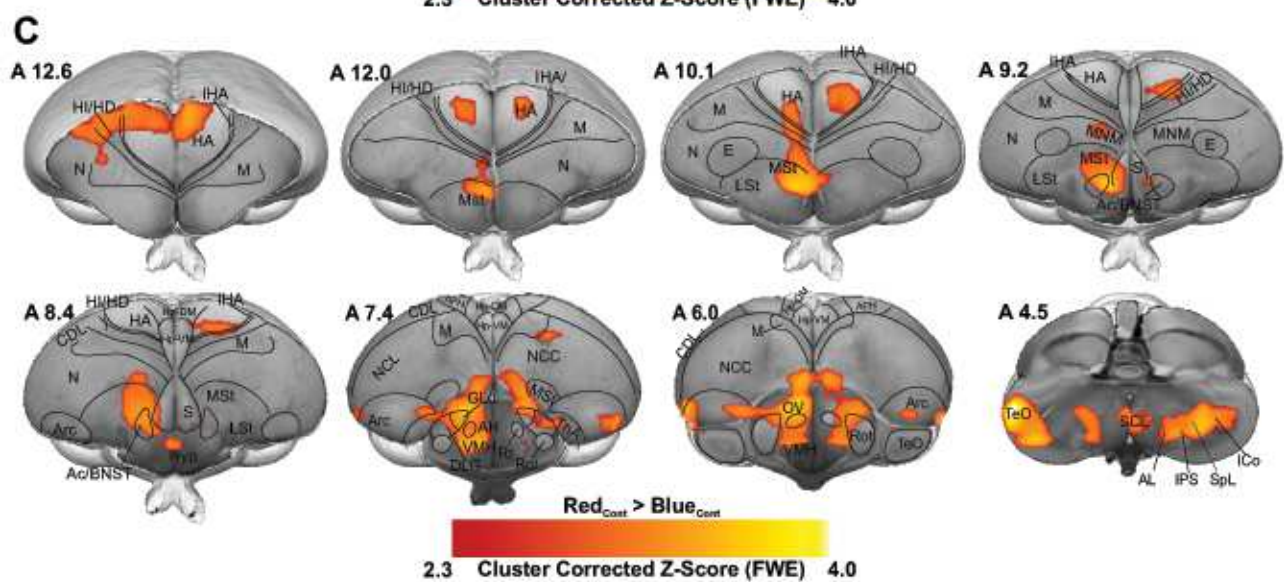
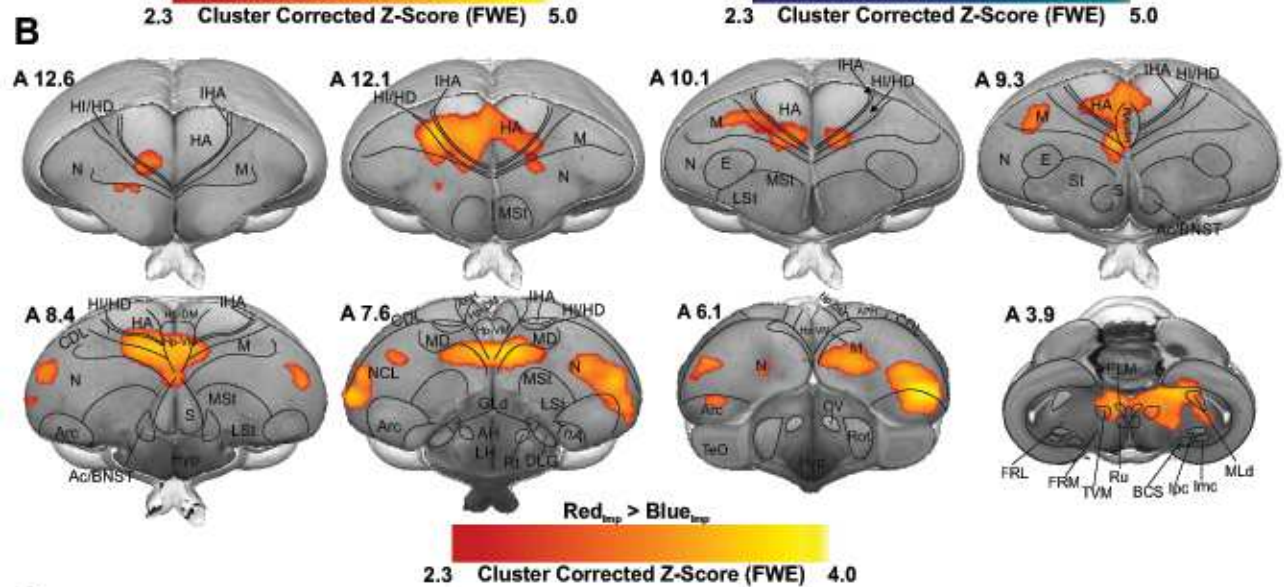
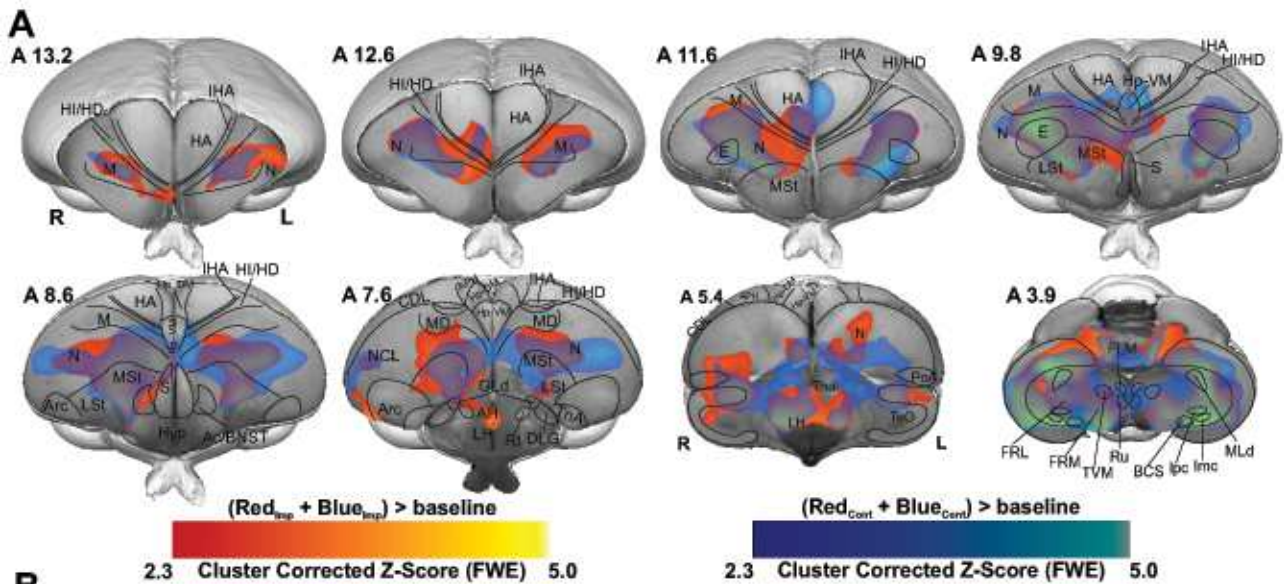
898 This index could range between 0 (absolute preference for the blue) and 1 (absolute  
899 preference for the red), whereas 0.5 represented the absence of preference between  
900 the two colours.

901 To estimate differences between the two imprinting groups we employed a two-tailed  
902 independent samples *t*-test. To estimate colour preference, we employed one-sample  
903 two-tailed *t*-test against chance (0.5).

904 To test the presence of differences in the colour preference between the two groups, we  
905 employed a two-tailed independent samples *t*-test. To verify the presence of a  
906 significant preference for either blue or red, we employed two-tailed one-sample *t*-test  
907 against chance (0.5).

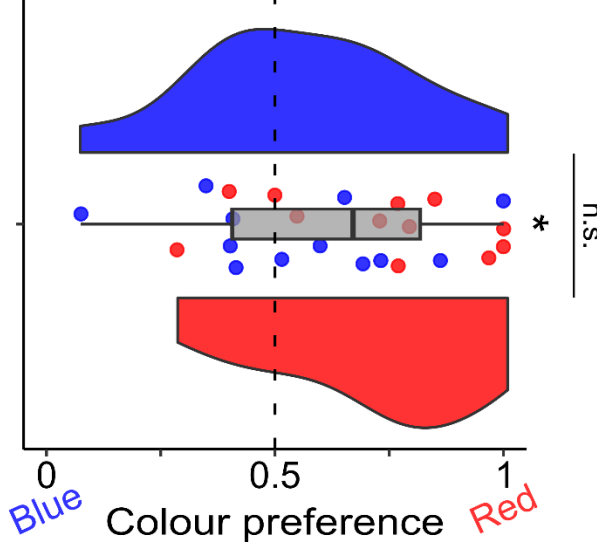
908

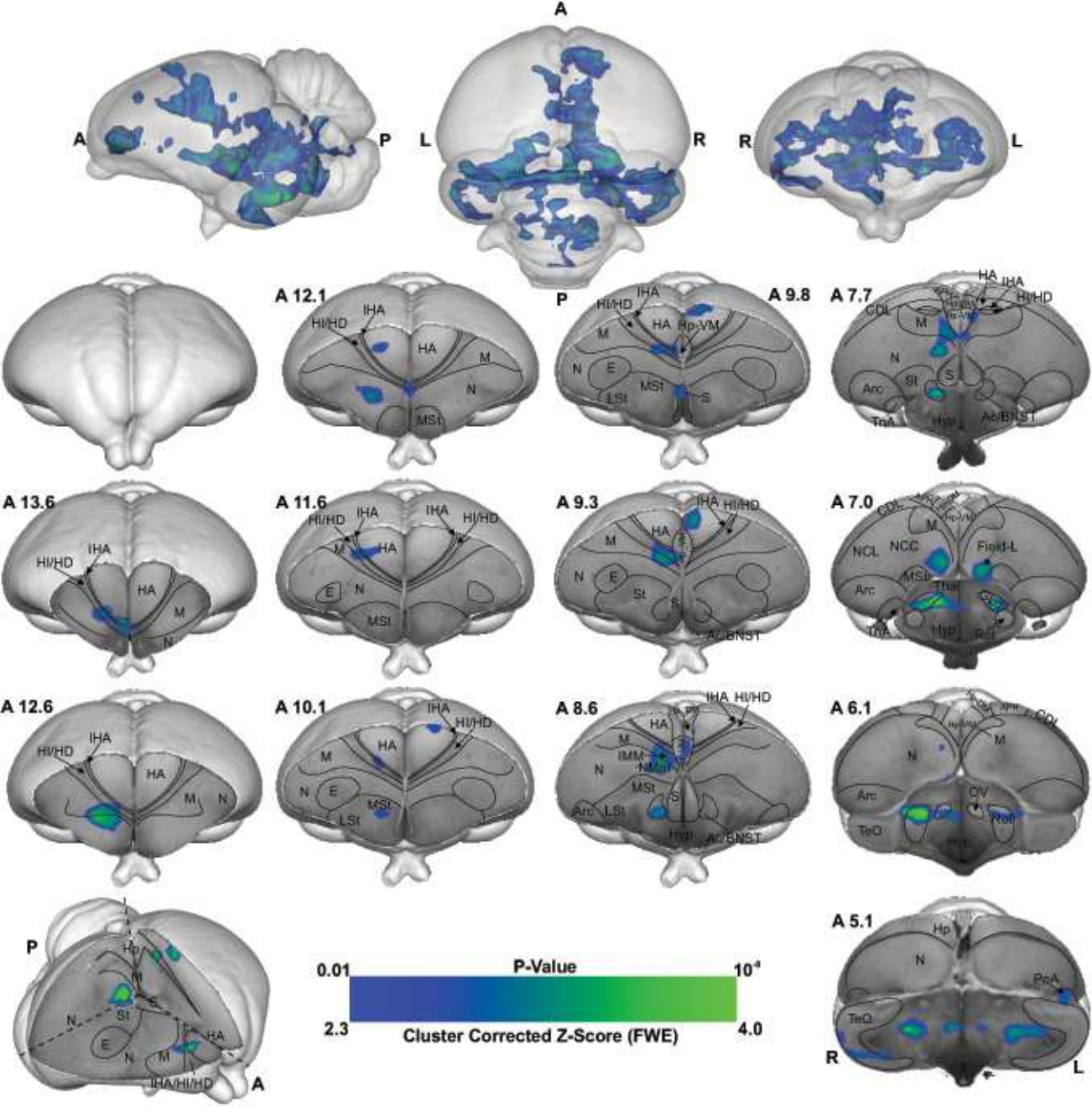




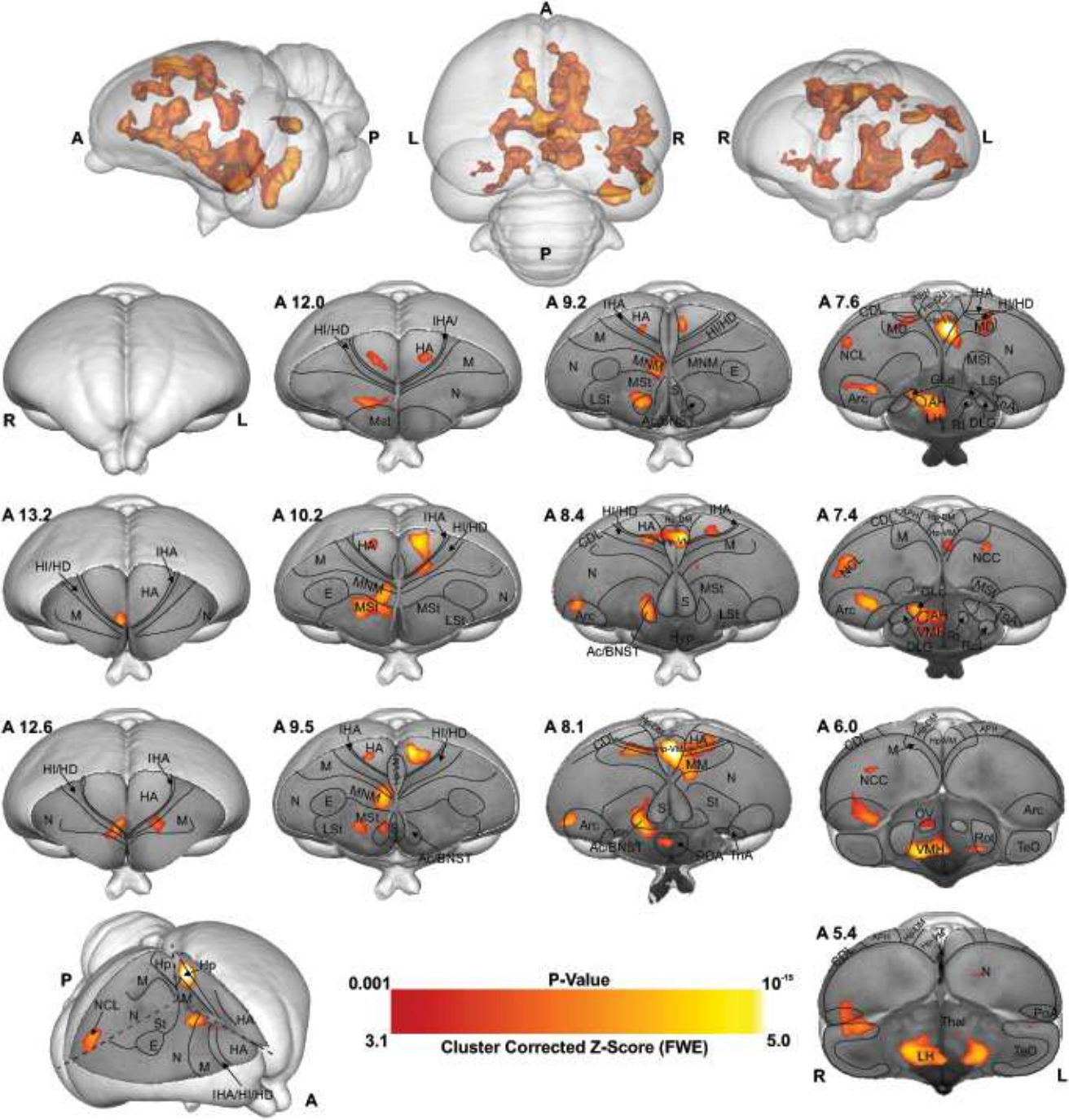
Imprinting

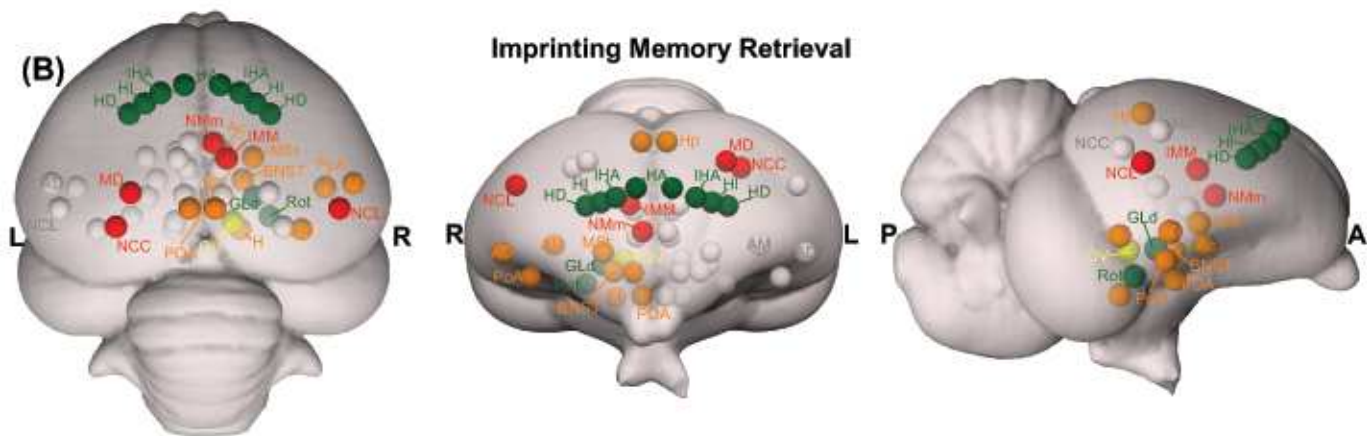
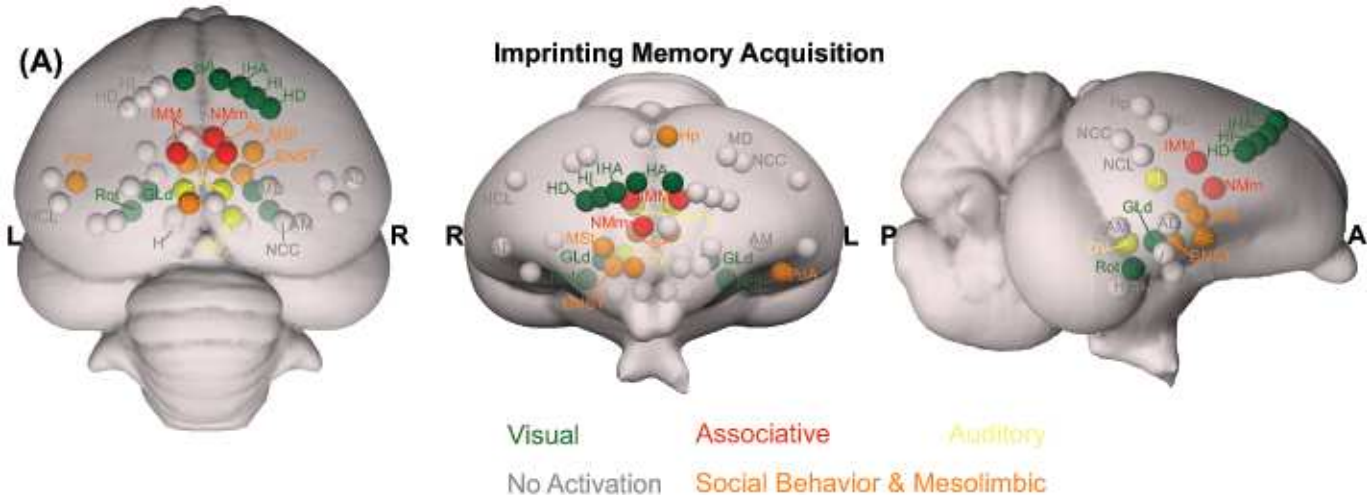
- Blue
- Red











## Supplementary Files

This is a list of supplementary files associated with this preprint. Click to download.

- [SupplementaryMaterialBehroozietal.pdf](#)